Available online at www.sciencedirect.com
SCIENCE DIRECT®
Journal of Catalysis 220 (2003) 382–391
JOURNAL OF CATALYSIS
www.elsevier.com/locate/jcat

In situ FTIR, EXAFS, and activity studies of the effect of crystallite size on silica-supported Pt oxidation catalysts

F.J. Gracia,[a] L. Bollmann,[a] E.E. Wolf,[a,*] J.T. Miller,[b] and A.J. Kropf[c]

[a] *Department of Chemical Engineering, University of Notre Dame, Notre Dame, IN 46556, USA*
[b] *BP Research Center, E-1F, 150 W. Warrenville Rd., Naperville, IL 60563, USA*
[c] *Chemical Technology Division, Argonne National Laboratory, 9700 S. Cass Avenue, Argonne, IL 60439, USA*

Received 18 March 2003; revised 27 June 2003; accepted 8 July 2003

Abstract

The effect of crystallite size on the activity of silica-supported Pt catalysts during CO oxidation has been investigated by kinetic studies and in situ infrared (IR) and extended X-ray absorption fine structure (EXAFS) spectroscopies. Catalysts containing 2% w/w Pt on silica were prepared by two different methods, rendering catalysts with dispersion values ranging between 0.29 and 0.80. Kinetic results indicate that the turnover frequency (TOF) of CO oxidation increases with increasing particle size under O_2-rich conditions, confirming that the CO oxidation reaction over Pt/SiO_2 catalysts is structure sensitive under an oxidizing environment. This characteristic is not only related to the gas phase surrounding the supported catalyst but also to the crystallite size range analyzed. EXAFS results show the formation of completely metallic Pt particles upon reduction in H_2 at 300 °C for 1 h regardless of the particle size, whereas after a subsequent oxidation pretreatment only the smallest particles are fully oxidized. At room temperature, the oxidized Pt surface does not adsorb CO, but under oxidizing conditions (1% CO, 10% O_2 in He) the oxidized catalysts show activity at $T > 100$ °C. Fourier-transform infrared spectroscopy indicates that even this low CO concentration leads to reduction of the oxidized surface under reaction conditions. The results presented here clearly show that the active surface of Pt/SiO_2 catalysts during CO oxidation is the metallic Pt, and that different sites on a Pt crystallite have different oxidation rates depending on its size. These results show the sensitivity of CO oxidation activity to the preparation method, pretreatment, and most significantly to the reaction atmosphere.

Keywords: Particle size effect; Pt/silica; CO oxidation; EXAFS; IR of adsorbed CO

1. Introduction

The average crystallite size and oxidation state of the surface are two of the most important parameters determining the activity of noble metal-supported catalysts. Boudart et al. [1] distinguished between catalytic reactions wherein the specific activity (moles/time/per active metal area) is independent of the active area (*facile* reactions) and those in which the specific activity changes with the specific area (*demanding* reactions). The traditional view for CO oxidation [2–11] is that this reaction is facile on noble metals at high CO partial pressures, where the reaction rate is negative order in CO concentration. In excess oxygen, however, the reaction rate is zero or positive order in CO concentration, and it has been found to be demanding. Several authors have reported particle-size effects on the various elementary steps involved in CO oxidation [12–17], as well as on the overall reaction rate (moles/second/mass catalyst) at both low and high CO concentrations [18–21]. Recently, the investigation of the reactivity of gold-supported catalysts has indicated that the highest activity during CO oxidation, even at room temperature, is obtained on samples with highly dispersed small gold particles [22–24]. In general, the role of particle size during oxidation reactions is not yet clear, as discrepancies may be found in the literature [25,26].

In many studies of oxidation reactions in our laboratory, dating back to the early 1980s [27–29], and more recently in our study of the role of Cl on Pt-supported catalysts [30], we have carefully measured reaction rates independent of mass transfer effects. In these studies, we have observed that the *conversion* and the *reaction rate per unit mass* were independent of Pt dispersion. Consequently, when reaction

* Corresponding author.
E-mail address: Eduardo.E.Wolf.1@nd.edu (E.E. Wolf).

0021-9517/$ – see front matter
doi:10.1016/S0021-9517(03)00296-3

rates are calculated per unit Pt area, i.e., as turnover number (TON) or turnover frequency (TOF), the catalysts with the *largest* Pt area (high dispersion) have the *lowest* TOF. What makes it difficult to determine uniquely the cause of this observation is that during oxidation reactions the reaction atmosphere contains oxygen. Hence, it is not clear whether the surface is metallic, oxidized, or a mixture of oxide and metallic phases [31,32]. Whereas this is true for supported Pd and Rh catalysts, in the case of Pt catalysts, we also found [30] that, as suggested by Burch and Loader [31b], platinum particles seem to have a strong "memory" of previous reduction pretreatments, as they remain in the metallic state under oxidizing conditions. We also showed that the active surface can be modified by the interaction of the precursor used during preparation (Cl) and the reactant mixtures under reaction conditions [30,33]. Since most surface analysis techniques are conducted under vacuum or ex situ, it is not always clear whether the same oxidation state is valid under reaction conditions at atmospheric pressure. Controlled-atmosphere EXAFS and in situ infrared (IR) spectroscopies are techniques that can be used under reaction conditions to probe the working surface. These techniques are used in this study, along with activity measurements, to demonstrate the relation between particle size and the oxidation state of the working surface during CO oxidation on Pt/SiO_2 catalysts.

2. Experimental

2.1. Catalyst preparation

Catalysts were prepared by adding tetraamineplatinum (+2) nitrate (PTA) to silica by two methods: wet impregnation, or adsorption (Ads), and incipient wetness impregnation (IWI). Impregnation was followed by calcination in flowing air at different temperatures to yield catalysts with identical Pt loading but different dispersions. To obtain catalysts with high dispersion, PTA was adsorbed on silica at a basic pH, whereas for catalysts with lower dispersion, PTA was added by incipient wetness impregnation with no adjustment in the pH.

2.1.1. Adsorption (Ads) of PTA

Fifty grams of silica (Davison grade 644, 300 m^2/g, 1.2 cc/g) were slurried in 400 mL H_2O. The pH was adjusted to 9.5 by addition of concn NH_4OH. Separately, 2.0 g of $Pt(NH_3)_4(NO_3)_2$ was dissolved in 50 mL of H_2O and added to the basic silica solution. Stirring was continued for an hour, and the solid was filtered. The solid was reslurried twice in 300 mL H_2O, filtered, and dried at room temperature and overnight at 100 °C. The Pt content was determined by ICP and was found to be 2.05% Pt. Portions of the catalyst were calcined at 100, 300, 400, 500, and 600 °C for 3 h.

Table 1
Catalyst preparation and Pt dispersion of reduced catalysts

Sample	% Pt	Method of preparation
1	2.0	Ads: calcined at 400 °C. No CO chemisorption at RT
2	2.0	Ads: calcined at 500 °C. No CO chemisorption at RT
3	2.0	Ads: calcined at 600 °C. No CO chemisorption at RT
4	2.0	IWI: calcined at 400 °C. No CO chemisorption at RT
5	2.0	IWI: calcined at 600 °C. No CO chemisorption at RT
6	2.0	Ads: calcined at 100 °C, reduced at 300 °C (H/Pt = 0.76)
7	2.0	Ads: calcined at 300 °C, reduced at 300 °C (H/Pt = 0.63)
8	2.0	IWI: calcined at 100 °C, reduced at 300 °C (H/Pt = 0.51)
9	2.0	IWI: calcined at 250 °C, reduced at 300 °C (H/Pt = 0.29)

2.1.2. Incipient wetness impregnation of PTA

Two grams of PTA were dissolved in 55 mL of H_2O (pH 5.5) and added to 50 g of Davison silica. The catalyst was dried at room temperature and overnight at 100 °C. Portions of the catalyst were calcined by heating at 1 °C/min to the final temperature of 100, 250, 400, and 600 °C and holding each temperature for 3 h.

The four samples calcined at temperatures up to 300 °C (samples 6–9) were further reduced in hydrogen for 1 h at 300 °C and evacuated for 15 min at the same temperature. Volumetric hydrogen chemisorption was determined at room temperature by the double isotherm method. The catalysts' methods of preparation and hydrogen chemisorption values (H/Pt) are given in Table 1.

2.2. Catalytic activity

Catalyst activities were determined using two types of reactors. A 10-port parallel microreactor (for high-throughput studies) was used first to determine the main effects of particle size and pretreatment for several samples in a single run. Then detailed kinetic information was obtained in a tubular-flow recycle microreactor.

The 10-port microreactor (ISRI, COMBI reactor [34]) was made of stainless steel and had 10 reaction wells (3/8 in. diameter, 2 in. long), each containing 200 mg of catalyst. The reactor was interfaced on-line through a multiple-port valve to a gas chromatograph (GC), which provided sequential composition analysis of the effluent from each of the 10 reaction wells. In some experiments, not all the 10 wells were used, and in such cases, silica was used in the empty wells to maintain the same flow distribution in each well. A valve was used as a restrictor at the exit of the total stream to maintain a constant pressure drop throughout each well and to equalize their flow. The catalyst particles were prepared by pressing the powders, breaking the resulting pellets, and sieving them between Nos. 18 and 30 Tyler meshes (1–0.6 mm size). The reactor system has programmable electronic flow controllers to meter the various gases into the reactor, with the total flow rate in each well maintained at 60 cc/min (total flow of 600 cc/min). The reactor was placed in a furnace equipped with a temperature control to maintain a constant reactor temperature, and several ther-

mocouples were used to measure the reactor temperature at different points.

The recycle reactor consisted of a quartz tube (12 in. long, 1/2 in. diameter) equipped with an external diaphragm pump to provide an external recycle loop. A thermocouple was placed in a thermowell in the center of the catalyst bed to monitor the temperature of the bed. The effluent flow rate was 130 cc/min, and the recycle ratio was about 20, to ensure complete mixing. The high flow rate through the catalyst bed (~ 26 L/min) assured the elimination of mass and heat-transport diffusional effects.

To stabilize the state of the surface and to ascertain the role of the oxidized vs the reduced surface prior to each run, the catalysts were pretreated either in air or H_2 at 200 °C for 3 h. The catalyst was then cooled to room temperature and switched to the reaction mixture, and the temperature was increased to about 200 °C. Catalyst activities were measured under diluted reactant concentrations: 1% CO in an oxidizing atmosphere with 10% O_2, balanced in He.

The product gases were analyzed by gas chromatography using a Molecular Sieve 5A column to separate CO and O_2 and a Hayasep Q column for CO_2, and a TC detector. The conversion data were reproducible within 5% accuracy or better for both the COMBI and the recycle reactors. Reaction rates were calculated at various temperatures at less than 5% conversion in the 10-port reaction and up to 20% conversion in the recycle reactor. Turnover frequencies were calculated from the rate and the dispersion values obtained for the freshly reduced catalysts and plotted vs $1/T$ to obtain activation energies.

2.3. EXAFS data collection and analysis

Measurements using extended X-ray absorption fine-structure (EXAFS) spectroscopy were made on the insertion-device beamline of the Materials Research Collaborative Access Team (MR-CAT) at the Advanced Photon Source, Argonne National Laboratory. Measurements were made in the transmission mode with ionization chambers optimized for the maximum current with linear response ($\sim 10^{10}$ photons detected/s). A cryogenically cooled double-crystal Si(111) monochromator was used in conjunction with a Rh-coated mirror to minimize the presence of harmonics [35]. Standard procedures based on WINXAS97 software [36] were used to extract the EXAFS data [37]. Phase shifts and backscattering amplitudes were obtained from EXAFS data for the reference compounds $Na_2Pt(OH)_6$ for Pt–O and Pt foil for Pt–Pt.

The sample was pressed into a cylindrical holder with a thickness chosen to give an absorbance ($\Delta\mu_x$) of about 1.0 in the Pt edge region, corresponding to approximately 100 mg of catalyst. The sample holder was centered in a continuous-flow in situ EXAFS reactor tube (18 in. long, 0.75 in. diameter) fitted at both ends with polyimide windows and valves to isolate the reactor from the atmosphere. The catalysts were pretreated in the laboratory by flowing gases or reactants at temperatures similar to those used during pretreatment or reaction. After the prescribed treatment, the sample was cooled to room temperature in the gas used for pretreatment or reaction, and then the cell was isolated by closing the valves fitted at both ends of the tube and moved to the X-ray hutch for measurement.

2.4. FTIR spectroscopy

Transmission infrared spectra of pressed disks (~ 14 mg) of Pt/SiO_2 were collected in situ in an IR reactor cell (ISRI, Inc.), placed in a Fourier-transform infrared (FTIR) spectrometer (Mattson, Galaxy 6020) at a resolution of 2 cm^{-1} and 30 scans/spectrum. The IR cell is equipped with NaCl windows, has connections for inlet and outlet flows, and thermocouples connected to a temperature controller to monitor and control the temperature. The spectra were obtained in the absorbance mode after subtraction of the background spectrum of the catalyst's disk under He atmosphere at the corresponding temperature. The samples were pretreated under various conditions prior to studying CO adsorption and reaction. After pretreatment, the catalyst was cooled to room temperature in He and 1% CO was added to the feed to measure CO adsorption. During the CO oxidation experiments, 10% O_2 was added to the CO-containing feed. In both experiments, the heating rate was 1 °C/min with a total flow of 120 cc/min.

3. Results

CO oxidation activity measurements were conducted to establish the differences in rate resulting from different pretreatments (calcination, reduction, and oxidation) for Pt on silica catalysts. Structural characterization of the initial state of the Pt in these catalysts was determined by EXAFS spectroscopy, and finally in situ FTIR studies were conducted for characterization of the catalysts under reaction conditions.

3.1. Activity measurements: the effect of calcination temperature

The CO conversion of samples 1–5 was measured to study the effect of the calcination temperature and preparation method on the activity. These samples were not reduced before reaction; instead, they were treated in situ in air at 200 °C for 2 h to normalize the state of the surface, even though they had been calcined previously in air at temperatures from 400 to 600 °C during preparation. A sample that was calcined and reduced during preparation (No. 9, $H/Pt = 0.29$) and was subsequently pretreated in air, i.e., oxidized, is included in Fig. 1 for comparison. The conversions as a function of temperature, measured in the parallel reactor, are shown in Fig. 1. The reaction rates of CO oxidation per unit mass of catalyst, calculated as differential rates at less than 5% conversion, are listed in Table 2.

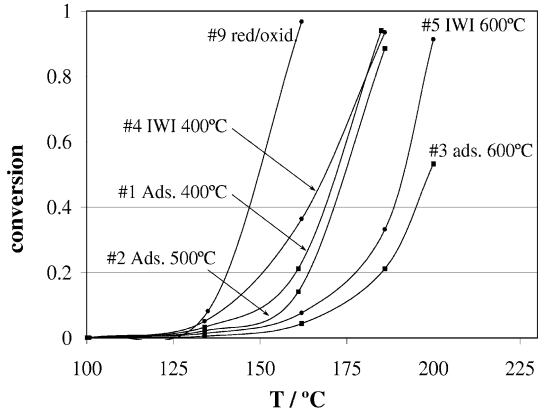

Fig. 1. Conversion vs temperature of Pt/SiO_2 catalysts calcined at different temperatures during preparation. Feed composition 1% CO, 10% O_2, balance He. Total flow rate 60 cc/min in a 10-port reactor.

Table 2
Reaction rate of calcined catalysts

Sample	Method of preparation	Reaction rate (mol CO_2/(s g_{cat}) $\times 10^9$)	
		130 °C	185 °C
1	Ads: calcined at 400 °C, reduced, H/Pt = 0.47[a]	5.76	147.63
2	Ads: calcined at 500 °C, reduced, H/Pt = 0.24[a]	3.85	139.07
3	Ads: calcined at 600 °C, reduced, H/Pt = 0.11[a]	0.93	32.01
4	IWI: calcined at 400 °C, reduced, H/Pt = 0.24[a]	9.13	150.61
5	IWI: calcined at 600 °C, reduced, H/Pt = 0.09[a]	2.49	54.07
9	IWI: H/Pt = 0.29, oxidized	14.04	147.56

[a] Chemisorption measured after reduction for 1 h at 300 °C.

The calcined samples (Nos. 1–5) were not active at $T <$ 125 °C but did show activity at higher temperatures. These results appeared inconsistent with the fact that there was no CO chemisorption at room temperature (RT) in the calcined samples. In all cases, however, the activity of the calcined samples was lower than that of the prereduced/oxidized catalyst (No. 9). Fig. 1 shows that the light-off temperature (LOT, i.e., temperature at 50% conversion) is similar for samples calcined at 400 and 500 °C (ca. 5 °C difference). For catalysts calcined at 600 °C, however, the LOT is about 25 and 50 °C higher than those of the 400 °C calcined (Nos. 1 and 4) and prereduced/oxidized (No. 9) catalysts, respectively.

Portions of the calcined samples 1–5 were later reduced in hydrogen at 300 °C for 1 h to measure their Pt dispersion. These values have been included in Table 2. After reduction, samples 2, 4, and 9 have nearly identical particle size based on their hydrogen chemisorption values. Thus, the differences in activity of these catalysts are not due only to differences in particle size, but the specific state of the Pt surface resulting from the different pretreatments. EXAFS characterization results, presented later on, helped to clarify this point.

Table 3
Reaction rate of (prereduced) Pt/SiO_2 catalysts with different pretreatments

Sample	H/Pt	Reaction rate (mol CO_2/(s g_{cat}) $\times 10^9$)			
		100 °C		130 °C	
		Calcined	Reduced	Calcined	Reduced
6	0.76	0.0	4.88	6.33	7.44
7	0.63	0.0	9.50	11.84	10.83
8	0.51	0.0	9.77	10.68	9.29
9	0.29	0.0	12.23	14.04	13.40

3.2. Activity measurements: the effect of particle size

The activities of the reduced catalysts, with dispersions ranging from 0.29 to 0.76 (samples 6–9), were measured in the 10-port reactor. The catalysts were pretreated prior to reaction in two ways: (a) oxidized at 200 °C in air for 3 h or (b) reduced in a 50% H_2–He mixture for 3 h at 200 °C. After pretreating, the CO conversion was determined from ambient to 200 °C using a slow linear ramp of 0.5 °C/min. Table 3 shows the rate per unit mass of catalysts at 100 and 130 °C. Fig. 2 shows the TOF, or rate per surface Pt atom, at each temperature.

The results in Fig. 2A and Table 3 show that, in agreement with Fig. 1, the oxidized catalysts exhibit no measurable activity below 100 °C, whereas the reduced catalysts (Fig. 2B) exhibit significant activity at these low temperatures. As the temperature increases above 100 °C, the rates per gram and TOFs of the catalysts pretreated by reduction or oxidation become similar. The implications are that, while the oxidized catalyst is initially inactive during the ramp in the reaction mixture, at higher temperature the surface undergoes a transformation and active Pt sites in the preoxidized and prereduced surfaces become the same. In other words, the surface is changed by the reactants as the temperature is increased to reaction temperature in the flowing reactant mixture.

Table 3 also shows that the rates per unit mass on the reduced catalysts at 100 °C and reduced and calcined catalysts at 130 °C are similar, even though there is more than a two-fold difference in the number of exposed Pt atoms between the low- and high-dispersion catalysts. Similar trends have been previously observed for several oxidation reactions [27,31a], i.e., the conversion seems to be similar even though the fraction of exposed Pt is quite different. From this, it follows that when the rate per unit mass is divided by the active area to calculate the TOF, significant differences in TOF are obtained. Fig. 2 shows a fivefold increase in the TOF as the dispersion decreases from 0.8 to 0.3.

The above results were obtained in the multiport, parallel plug-flow reactor at low conversion, and thus are subject to some analytic error. The characteristic autothermal behavior of the plug-flow reactor further limits the conversion, and the potential presence of micro-hot spots can further increase the error in measuring activation energies. To obtain more accurate kinetic data devoid of heat and mass-transfer effects, the rates of CO oxidation were determined for the reduced catalysts in the recycle reactor.

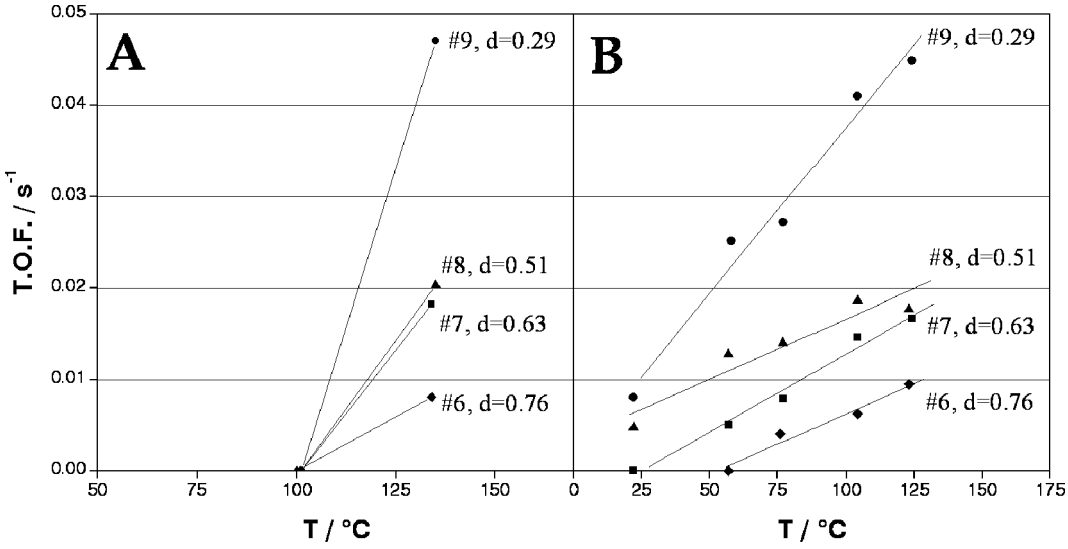

Fig. 2. TOF for CO oxidation on reduced Pt/SiO_2 catalysts with different dispersions. Pretreatment: (A) oxidation in air or (B) reduction in H_2 at 200 °C. Feed composition 1% CO, 10% O_2, balance He. Total flow rate 60 cc/min in a 10-port reactor.

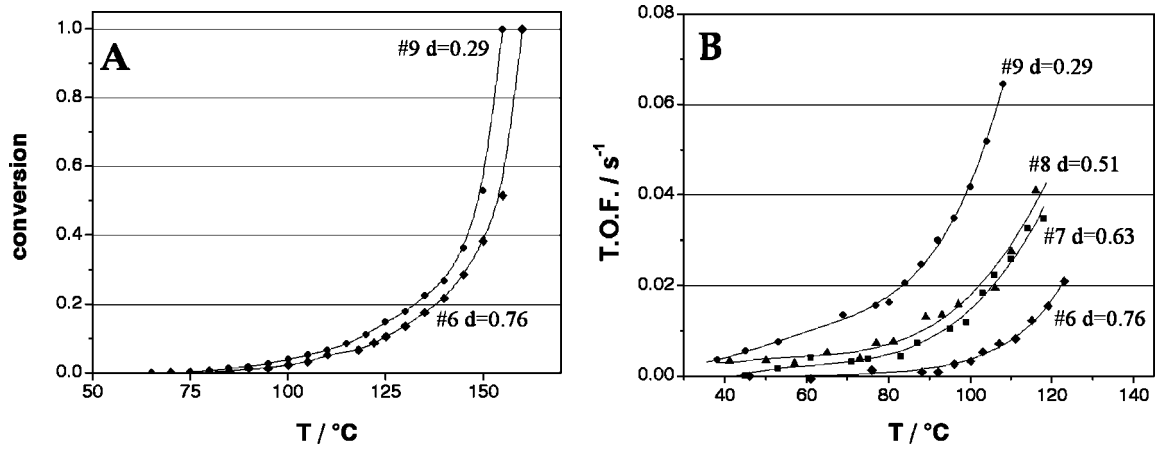

Fig. 3. CO oxidation on (prereduced) Pt/SiO_2 catalysts with different dispersions. (A) Conversion vs temperature; (B) TOF vs temperature, using a recycle reactor.

The fractional CO conversion in the recycle reactor (Fig. 3A) shows again that as in the 10-port parallel reactor, the conversion is quite similar for the two catalysts having very different dispersion; consequently, the TOF of the low-dispersion catalyst (low Pt area) is the highest (Fig. 3B). The different conversion–temperature curves obtained in the 10-port reactor vs the recycle reactor are due to the better heat-transfer characteristics and more isothermal conditions of the recycle reactor and the higher accuracy of the GC readings at higher conversion. Because of the absence of temperature gradients, which might cause microlocalized heating in the parallel reactor, the LOT is higher in the recycle reactor.

The Arrhenius plot (Fig. 4) shows that the apparent activation energy decreases as the dispersion of the Pt/SiO_2 catalysts decreases. These results clearly show that CO oxidation on small Pt crystallites is a structure-sensitive reaction. It should be noted that these differences in activation

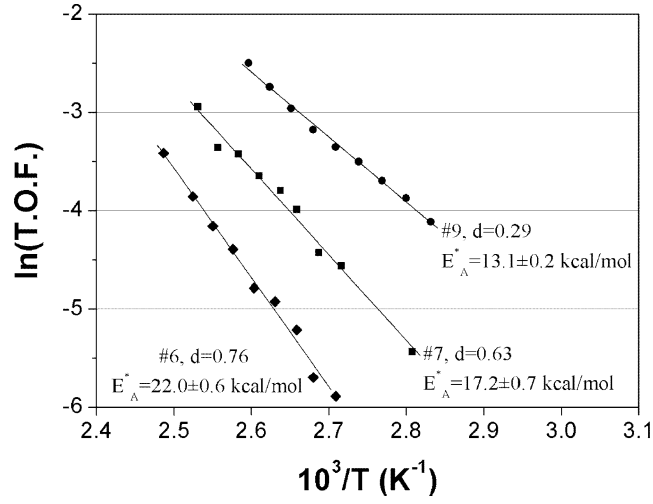

Fig. 4. Arrhenius plot of Pt/SiO_2 catalysts with different dispersions.

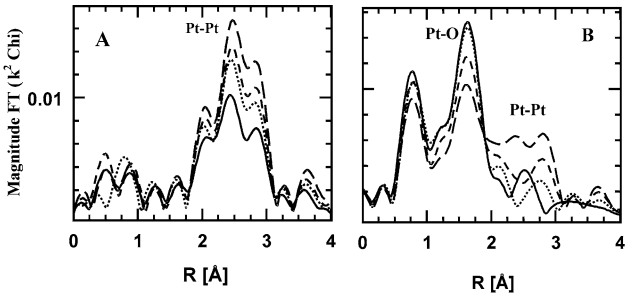

Fig. 5. Fourier transform of (A) reduced and (B) oxidized Pt/SiO_2 catalysts with different dispersions: solid, sample 6 (H/Pt = 0.76); dotted, sample 7 (H/Pt = 0.63); dashed, sample 8 (H/Pt = 0.51); and long dash, sample 9 (H/Pt = 0.29).

energy were not distinguishable from the conversion data obtained in the 10-port reactor. The low conversion required to obtain differential rates in the 10-port reactor does not permit accurate evaluation of the apparent activation energy (E^*_A).

3.3. EXAFS characterization

The EXAFS and X-ray absorption near-edge structure (XANES) data were obtained under a controlled atmosphere at room temperature after the catalysts were pretreated (either in air or hydrogen) prior to data collection in the EXAFS cell. The XANES spectra (not shown) indicate that with increasing calcination temperature of the silica impregnated with PTA, there is an increase in the white-line intensity and a shift of the edge threshold to lower energy, which is indicative of oxidation of Pt^{2+} to Pt^{4+}. For the catalyst prepared by incipient wetness impregnation, oxidation is complete at 250 °C, while for the catalyst prepared by adsorption, approximately 75% is oxidized to Pt^{4+} at 400 °C. The Fourier transforms for Pt adsorbed on silica and calcined at 400, 500, and 600 °C indicate that at temperatures below 400 °C, there is a large peak at about 1.6 Å, characteristic of Pt–O [38,39], indicating that the Pt is nonmetallic. As the calcination temperature increases above 500 °C, however, increasing amounts of metallic Pt are observed.

The effect of reduction and oxidation on the structure of the Pt is shown in Fig. 5 in terms of magnitude of the Fourier transform (FT) of the EXAFS signal. It should be noted that the magnitude of the Fourier transform is not a radial distribution function. The peak position does not equal the bond length, and the number of peaks is not an indication of multiple bond distances. The peak position is altered by the oscillatory component of the phase shift in the EXAFS signal. As a result, a single bond distance such as Pt–Pt can exhibit multiple peaks in the FT magnitude, due to multiple peaks in the backscattering amplitude as a function of the electron momentum. Reduction in H_2 at 300 °C for 1 h (Fig. 5A) gives multiple peaks around 2.5 Å corresponding to Pt–Pt bonds, with the magnitude of the FT increasing with decreasing dispersion, as expected. The EXAFS fits for the reduced catalysts are given in Table 4. The Pt–Pt bond distance of these reduced catalysts with dispersions from 0.76 to 0.29 are slightly shorter (2.75 Å) than that in Pt foil (2.77 Å) and are consistent with small particles [40,41].

Table 4
EXAFS fits of reduced and oxidized Pt/SiO_2 catalysts with different dispersions

Sample	H/Pt	Back scatter	CN	DWF		
				R (Å)	($\times 10^3$)	E_o (eV)
Reduced at 300 °C						
6	0.76	Pt–Pt	5.0	2.75	1.0	−3.4
7	0.63	Pt–Pt	6.6	2.75	1.0	−2.6
8	0.51	Pt–Pt	7.3	2.76	1.0	−1.7
9	0.29	Pt–Pt	8.8	2.76	1.0	−1.5
Oxidized at 200 °C						
6	0.76	Pt–O	3.7	2.06	0.8	1.4
7	0.63	Pt–O	3.6	2.06	0.8	1.0
		Pt–Pt	1.3	2.74	0.7	−1.1
8	0.51	Pt–O	3.1	2.05	0.8	1.6
		Pt–Pt	2.2	2.73	0.7	−3.6
9	0.29	Pt–O	2.7	2.05	0.8	1.5
		Pt–Pt	3.7	2.74	0.7	−2.9

The reduced catalysts were oxidized in a 4% O_2/He mixture at 200 °C. The magnitude of the FT (Fig. 5B) indicates that there is a mixture of oxidized and reduced Pt. In addition, the fraction of oxidized Pt is dependent on the particle size. For example, the most highly dispersed catalyst (No. 6, H/Pt = 0.76) is completely oxidized, while the fraction of oxidized Pt decreases with increasing particle size.

The fits of the EXAFS data for the oxidized catalysts are also given in Table 4. The Pt–O coordination number of sample 6 (H/Pt = 0.76) is near 4 (with no remaining Pt–Pt), suggesting that the Pt is oxidized to Pt^{2+}. Although sample 9 (H/Pt = 0.29) has reduced particles of about 30–40 Å, oxidation was incomplete. This suggests that oxidation of metallic Pt is limited to a few surface layers. The Pt–Pt bond length is slightly shorter that of Pt foil, which is similar to that observed for the reduced particles. Upon re-reduction of the oxidized particles, the hydrogen chemisorption values and EXAFS are identical to that of the reduced particles, indicating no sintering of the particles when oxidized at below 200 °C.

In summary, the EXAFS results show that calcined catalysts are fully oxidized when calcined below 400 °C, but higher calcination temperatures lead to formation of metallic Pt. The amount of metallic Pt increases with increasing calcination temperature. Hydrogen reduction leads to fully metallic particles. The dispersion decreases as the calcination temperature increases. The calcined and oxidized catalysts do not adsorb CO at room temperature, indicating no exposed metallic Pt. Nonetheless, the results shown in Sections 3.1 and 3.2 indicate that both calcined and oxidized samples can oxidize CO at temperatures above 100 °C. To analyze this apparent contradiction in more detail, several samples were studied using in situ FTIR during reaction conditions.

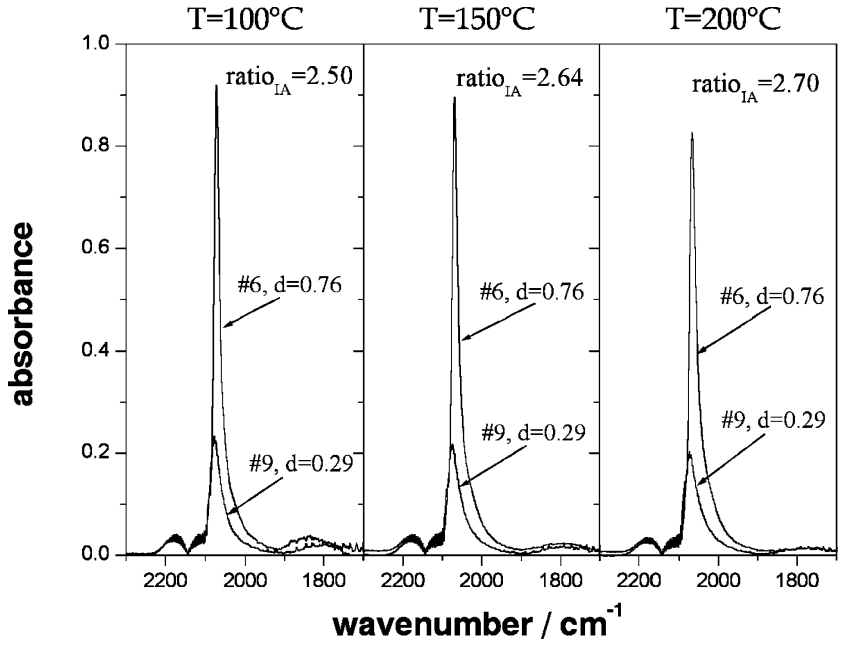

Fig. 6. IR spectra of adsorbed CO on reduced Pt/SiO_2 catalysts No. 6 (H/Pt = 0.76) and No. 9 (H/Pt = 0.29). Feed composition 1% CO in He. Total flow rate 120 cc/min.

3.4. Temperature-programmed in situ FTIR

3.4.1. CO adsorption

FTIR absorbance spectra of adsorbed CO on the reduced catalysts No. 6 (H/Pt = 0.76) and No. 9 (H/Pt = 0.29) at 100, 150, and 200 °C are shown in Fig. 6. As expected, there is a smaller CO band on the catalysts with lower dispersion. For both catalysts, the band's intensity slightly decreases with increasing temperature, from 100 to 200 °C, due to a small amount of CO desorption. Although the ratio of integrated CO absorbances (IA) is similar to the H/Pt ratios of both catalysts (2.7), with increasing temperature, there is a small increase in the IA ratio, e.g., from 2.5 to 2.64 to 2.7. This is due to the slightly greater percentage of CO desorption on the catalyst with lower dispersion.

When similar experiments were conducted with oxidized catalysts, *no CO adsorption* was observed at RT, indicating no exposed metallic Pt. However, upon increasing the temperature in flowing CO to 100 °C, the CO absorbance of sample 6 increased to approximately 50% of the absorbance of the reduced catalyst and the intensity of the band increased with time on stream. After 30 min, the difference in the CO IA between the oxidized and the reduced catalyst was only about 15%. At the end of the run ($T = 200$ °C, 90 min), there was *no difference* between the intensity of the CO band for the calcined and reduced catalysts. This shows that at $T > 100$ °C, CO completely reduced the oxidized catalyst's surface to metallic Pt.

3.4.2. CO–O_2 reaction

Similar FTIR measurements were conducted on reduced Pt/silica, samples 6 and 9 (H/Pt = 0.76 and 0.29, respectively), but now in the presence of the same reactant gas composition (1% CO, 10% O_2, balance He) as during the activity measurements, i.e., under an oxidizing stream. On the reduced catalysts, the intensity of the adsorbed CO band under the reaction mixture was identical to that observed in the presence of only CO gas (i.e., as in Fig. 6). At the ignition temperature (around 160 °C), however, there was a sudden decrease in CO absorbance, reaching a value below the IR detection limit. Concurrently, there is a sudden increase in the amount of gas-phase CO_2. This behavior, while not shown here, exemplifies the Langmuir–Hinshelwood oxidation mechanism, and is similar to that reported in previous IR studies [28,30]. After ignition, the CO flow was discontinued while maintaining the 10% O_2 flow for 90 min at 200 °C; thus, the surface was expected to become oxidized again. After decreasing the temperature to 100 °C, the feed was switched again to the CO/O_2 reactant gas mixture. The CO absorbance observed after the switch, however, was identical to that of the reduced catalysts, indicating that the surface was quickly reduced when the flow was resumed, even under an oxidizing atmosphere (1% CO, 10% O_2, He).

The IR spectra of Pt/silica calcined at 400 °C (sample 4, in Table 1) were also obtained after exposure of CO/O_2 at different temperatures. This sample, according to the EXAFS results (see Table 4), initially contains no metallic Pt. The IR results (Fig. 7) accordingly show no CO adsorption at room temperature. At 100 °C, however, there is a small broad band at 2105 cm^{-1}. As the temperature increases, however, a band at 2077 cm^{-1}, corresponding to linearly adsorbed CO on metallic Pt, begins to increase while the band at 2105 cm^{-1} decreases. At the same time, small amounts of gas-phase CO_2 are observed. The amount of metallic Pt from the CO absorption band correlates well with the activity of this catalyst, as shown in Fig. 1. Ignition starts

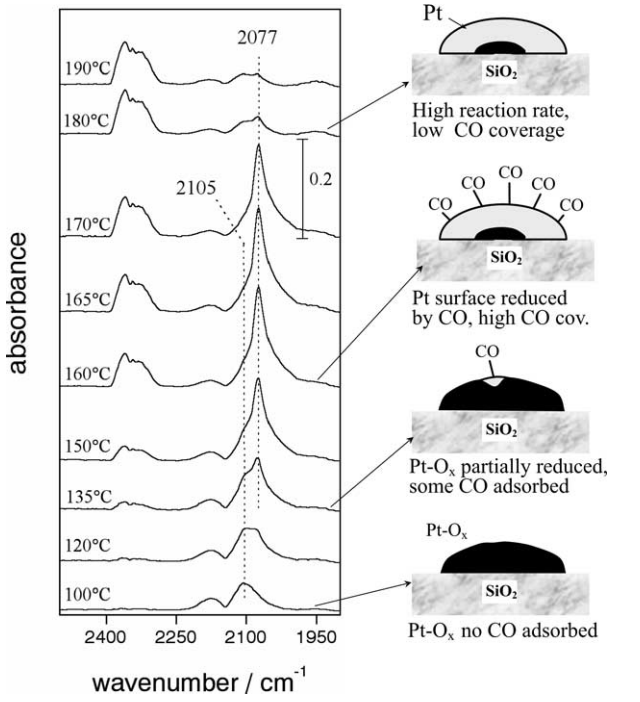

Fig. 7. IR spectra of 400 °C calcined Pt/SiO_2 (sample 4) during CO oxidation. Feed composition 1% CO, 10% O_2, balance He. Total flow rate 120 cc/min.

at about 160 °C, but it is not as abrupt as that for the reduced samples. Above 180 °C, the surface coverage of CO is low. A cartoon depicting these IR results is displayed on the right of Fig. 7. Initially, the fully oxidized surface adsorbs small amounts of CO. As the temperature increases, despite the large excess of O_2, the surface starts getting reduced, perhaps by an Eley-Rideal mechanism. The oxidized Pt surface continues to reduce at higher temperatures. At about 150 °C, the Pt particles' surface is fully reduced with a high CO coverage. As the temperature increases further, the rate of CO oxidation increases and CO coverage decreases, as in the case of the reduced catalyst. In other words, as shown by the activity results, the state of the surface is dictated by the reaction environment. Contrary to expectations, flowing a net oxidizing mixture containing 1% CO over the Pt surface actually does not result in an oxidized surface, but instead in a reduced surface. Obviously, these results will vary depending on the concentration of oxygen and CO in the feed.

4. Discussion

The model that emerges for CO oxidation is that, even in the presence of an oxygen-rich mixture, the active surface is metallic Pt. The EXAFS analysis of the catalysts calcined near 400 °C are predominantly Pt^{4+} oxide before reaction. Although oxidized Pt is initially inactive at low temperature (< 100 °C), the activity becomes equivalent to that of reduced Pt at $T > 100$ °C. The FTIR results show that CO is not adsorbed on oxidized Pt at low temperatures. With increasing temperature, however, oxidized Pt is reduced by CO even with a large excess of O_2. Thus, while metallic Pt is readily oxidized by pure O_2 at reaction temperatures, the presence of low CO concentrations is sufficient to reduce the oxidized Pt surface.

Herz and Shinouskis reported similar IR results on a Pt/Al_2O_3 catalyst [42]. These authors observed a rapid shift of an IR band from 2120 to 2070 cm^{-1} as the reactant mixture is switched from a 1% O_2/He mixture at 250 °C to a 1% CO/He. In another IR study on a Pt/Al_2O_3 catalyst Anderson [43] also reported the presence of a carbonyl species band at 2125 cm^{-1}. This author attributes this band to CO adsorbed at Pt^{2+} sites coexisting with metallic Pt and indicates that this species is unreactive in the presence of oxygen at temperatures between 200 and 300 °C.

This study clearly confirms previous results showing that on highly dispersed (reduced) catalysts, the rate per unit mass is similar to that of catalysts with low dispersion (Fig. 3A). The resulting corollary is that the turnover number, TON, increases with decreasing particle size (Fig. 3B); i.e., the activity per surface Pt increases with increasing particle size. Careful kinetic results obtained in a recycle reactor showed that the apparent activation energy also decreases slightly as the particle size increases. It follows that changing particle size not only changes the number of Pt sites, but also changes the activity per site, clearly showing the structure sensitivity of the CO oxidation reaction.

For CO-rich conditions, where the catalytic surface is mostly covered by CO and the reaction rate is inverse order with respect to the CO partial pressure, CO oxidation has been found to be structure insensitive on Pd(100), Pd(110), Pd(111) [3], Pd/α-Al_2O_3 [6,7], Rh/α-Al_2O_3, Rh/SiO_2, Rh/θ-Al_2O_3 [8,9], Pt/SiO_2, and Pt/Al_2O_3 [4,11]. On the other hand, under O_2-rich conditions, CO oxidation is reported to be a demanding, or structure-sensitive, reaction on various catalysts from single crystals [12,19] to model catalysts with small Pd or Pt clusters supported on flat supports [16,19,21], to supported catalysts [2,18,27], similar to the results presented in Section 3.2.

Despite the above results, less attention has been given to highly dispersed oxidation catalysts. Akubuiro et al. [18] analyzed zeolite Y-supported Pt catalysts with particle sizes ranging between 18 and 1000 Å. They found that for both high and low CO concentrations (0.3 and 2% CO, CO/O_2 ratio = 0.45), the TOF increased as the particle size increased up to approximately 30 Å. At high CO concentrations, the activity remained constant with larger particle sizes. For low CO concentrations, there was a small decrease in the TOF between 30 and 50 Å, with no other changes in activity for larger particles.

The previous results for CO oxidation may be categorized into three groups. Several studies have been conducted on large particles, generally larger than 25 Å under stoichiometric reaction conditions. In this case, CO oxidation is *facile*, or the TON is independent of particle size [2,6–11]. Several studies have also been made on metal particles between

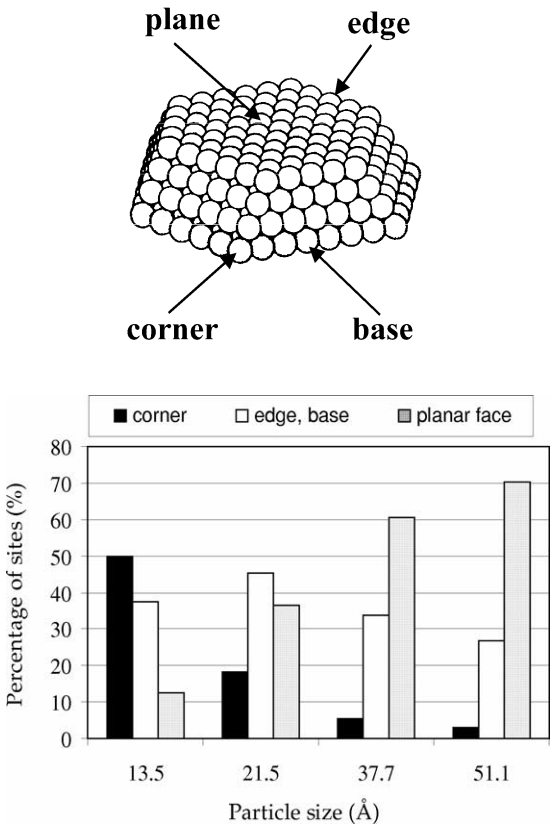

Fig. 8. Crystallite model used for Monte Carlo simulations. Pt crystallite model and proportion of sites for different Pt particle sizes.

about 10 and 60 Å, also under stoichiometric conditions [5], and with crystallites between 30 and 75 Å [17,44]. For these catalysts, there is only a small change in the TON with particle size. Finally, a number of studies have shown that on small metal particles, generally, less than about 20 Å, CO oxidation is structure sensitive under both CO-rich and CO-lean conditions [13,15b,18,20,21,45]. The present study, with particles between 10 and 40 Å, is similar in size to the third group. The reaction conditions were highly oxidizing, i.e., CO lean.

To explain the change in intrinsic activity with size, we need to consider a model of a Pt crystallite such as the one depicted in Fig. 8. Such a model has been proposed by Mavrikakis [46] and was used in our Monte Carlo simulation studies of the CO oxidation reaction [47,48]. As the size of the particle changes, the ratio of Pt atoms at the corner, edge, and flat surfaces will change, and we can calculate the number of these atoms for different crystallite sizes (Fig. 8).

As the crystallite size increases, the fractions of Pt atoms at low coordination sites, i.e., corners and edges, decrease dramatically while the fraction of atoms on planer faces increases with a relatively small increase in the particle size. For an average size of 14 Å, for example, the fraction of Pt atoms in planer surfaces is only 12.5%, whereas for a particle of 38 Å, more than 60% of surface atoms are on planar faces.

Since a detailed description of the Monte Carlo simulations is beyond the scope of this paper, only the main results are presented next. Using the crystallite model presented in Fig. 8, supported catalysts with dispersions 0.29 and 0.80 were considered in the simulations. For each catalyst, the number of crystallites on the support was varied in order to maintain the *total number* of metal atoms constant. This is equivalent to analyzing catalysts with different dispersion but the same metal loading. Initially, the TOFs of both catalysts were calculated assuming that the rates of adsorption, surface reaction, and desorption were the same in corner, edges, and plane sites. In this case, it was not possible to fit the experimental data to the theoretical results, since the simulation yielded that both supported catalysts have the same overall activity.

We found that the experimental rates agree with the theory *only* when the rate of surface reaction on low coordination Pt, i.e., corners, edges, etc., is at least 10 times smaller than that on the planar faces. This is reasonable if one considers that at corner and edge sites the more strongly adsorbed reactants must overcome an additional energy barrier to diffuse and react, thus lowering the rate of surface reaction in these sites. Based on transient kinetic experiments on a Pt(112) single crystal, Szabó et al. [14] found that CO on Pt plane surfaces is more reactive than when adsorbed at step sites. Siera et al. confirmed this conclusion for CO oxidation on Pt–Rh (111), (100), (410), and (210) single crystal surfaces [49]. These authors report that CO oxidation occurs at a relative low temperature on flat surfaces, but at a higher temperature on stepped surfaces. As the Monte Carlo simulations indicate, for large particles there is only a small increase in the number of more reactive planer atoms with increasing particle size, and this is offset, at least in part, by the loss in dispersion. Therefore, little change in the TON is expected for larger particles, as was observed. All studies, therefore, are consistent with the interpretation that flat surfaces have a significantly higher CO oxidation activity compared to low coordination edge and corner atoms.

5. Conclusions

Two different methods have been used to prepare silica-supported Pt catalysts with different dispersions. Calcined or oxidized catalysts do not adsorb CO at room temperature, but at $T > 100\,^{\circ}\mathrm{C}$ these catalysts show activity during CO oxidation. In situ FTIR results clearly indicate that metallic Pt is the active phase of Pt/SiO_2 catalysts. A model has been proposed to describe the changes in the catalytic surface upon exposure to CO, even at low concentrations. These changes lead to reduction of the oxidized surface, allowing CO adsorption and the subsequent reaction with adsorbed oxygen.

Kinetic studies complemented with EXAFS and in situ IR results confirmed that, under O_2-rich conditions, the CO oxidation reaction is structure sensitive on Pt/SiO_2 catalysts,

as the specific activity (TOF) increases with increasing particle size. The reason for this structure sensitivity is likely to be the difference in activity of catalytic sites present on flat surfaces compared to that of low coordination sites, like edges or corners. Because the relative proportion of planar, step, and corner sites in a crystallite depends on its size, the activity for CO oxidation of a silica-supported Pt catalyst is affected by the average particle size, especially for catalysts with small crystallites or high dispersions.

Acknowledgments

Use of the Advanced Photon Source was supported by the U.S. Department of Energy, Office of Basic Energy Sciences, Office of Science (DOE-BES-SC), under Contract No. W-31-109-Eng-38. The MR-CAT is funded by the member institutions and DOE-BES-SC under Contracts DE-FG02-94ER45525 and DE-FG02-96ER45589. We also acknowledge funding of this work from NSF CTS 01 38070 grant.

References

[1] M. Boudart, A. Aldag, J.E. Benson, N.A. Dougharty, C.G. Harkins, J. Catal. 6 (1966) 92–99.
[2] E. McCarthy, J. Zahradnik, G.C. Kuczynski, J.J. Carberry, J. Catal. 39 (1975) 29–35.
[3] T. Engel, G. Ertl, Adv. Catal. 28 (1979).
[4] N.W. Cant, J. Catal. 62 (1980) 173–175.
[5] N.W. Cant, R.A. Donaldson, J. Catal. 71 (1981) 320–330.
[6] S. Ladas, H. Poppa, M. Boudart, Surf. Sci. 102 (1981) 151–171.
[7] L. Kieken, M. Boudart, in: L. Guczi, et al. (Eds.), New Frontiers in Catalysis: Proceedings 10th International Congress on Catalysis, Elsevier, Amsterdam, 1993, pp. 1313–1324.
[8] S.H. Oh, G.B. Fisher, J.E. Carpenter, D.W. Goodman, J. Catal. 100 (1986) 360–376.
[9] S.H. Oh, C.C. Eickel, J. Catal. 128 (1991) 526–536.
[10] C. Wong, R.W. McCabe, J. Catal. 119 (1989) 47–64.
[11] D.R. Rainer, M. Koranne, S.M. Vesecky, D.W. Goodman, J. Phys. Chem. B 101 (1997) 10769–10774.
[12] H. Hopster, H. Ibach, G. Comsa, J. Catal. 46 (1977) 37–48.
[13] D.N. Belton, S.J. Schmieg, Surf. Sci. 202 (1988) 238–254.
[14] A. Szabó, M.A. Henderson, J.T. Yates, J. Chem. Phys. 96 (8) (1992) 6191–6202.
[15] (a) G.S. Zafiris, R.J. Gorte, Surf. Sci. 276 (1992) 86–94;
(b) G.S. Zafiris, R.J. Gorte, J. Catal. 140 (1993) 418–423.
[16] I. Meusel, J. Hoffmann, J. Hartmann, J. Libuda, H.J. Freund, J. Chem. Phys. B 105 (2001) 3567–3576.
[17] A.K. Santra, D.W. Goodman, Electrochim. Acta 47 (2002) 3595–3609.
[18] E.C. Akubuiro, X.E. Verykios, L. Lesnick, Appl. Catal. 14 (1985) 215–227.
[19] I. Stará, V. Nehasil, V. Matolín, Surf. Sci. 331–333 (1995) 173–177.
[20] V. Nehasil, I. Stará, V. Matolín, Surf. Sci. 352–354 (1996) 305–309.
[21] U. Heiz, A. Sanchez, S. Abbet, W.D. Schneider, J. Am. Chem. Soc. 121 (1999) 3214–3217.
[22] (a) M. Haruta, Catal. Today 36 (1997) 153–166;
(b) M. Haruta, Cattech 6 (2002) 102–115.
[23] J. Grunwaldt, C. Kiener, C. Wögerbauer, A. Baiker, J. Catal. 181 (1999) 223–232.
[24] A. Wolf, F. Schüth, Appl. Catal. A 226 (2002) 1–13.
[25] D.W. Goodman, C.H.F. Peden, G.B. Fisher, S.H. Oh, Catal. Lett. 22 (1993) 271–274.
[26] M. Bowker, Q. Guo, Y. Li, R.W. Joyner, Catal. Lett. 22 (1993) 275–276.
[27] L.M. Carballo, E.E. Wolf, J. Catal. 53 (3) (1978) 366–373.
[28] D.J. Kaul, R. Sant, E.E. Wolf, Chem. Eng. Sci. 42 (6) (1987) 1399–1411.
[29] G.S. Lane, E.E. Wolf, J. Catal. 105 (2) (1987) 386–404.
[30] F.J. Gracia, J.T. Miller, A.J. Kropf, E.E. Wolf, J. Catal. 209 (2) (2002) 341–354.
[31] (a) R. Burch, P.K. Loader, Appl. Catal. B 5 (1994) 149–164;
(b) R. Burch, P.K. Loader, Appl. Catal. A 122 (1995) 169–190.
[32] S. Yang, A. Maroto-Valiente, M. Benito-Gonzalez, I. Rodriguez-Ramos, A. Guerrero-Ruiz, Appl. Catal. B 28 (2000) 223–233.
[33] A. Berkó, G. Ménesi, F. Solymosi, J. Phys. Chem. 100 (1996) 17732–17734.
[34] W. Li, F.J. Gracia, E.E. Wolf, Catal. Today (2003), in press.
[35] C.U. Segre, N.E. Leyarovska, W.M. Lavender, P.W. Plag, A.S. King, A.J. Kropf, B.A. Bunker, K.M. Kemmer, P. Dutta, R.S. Duran, J. Kaduk, in: P. Pianetta, et al. (Eds.), Proceedings of CP521, Synchroton Radiation Instrumentation: 11th U.S. National Conference, Amer. Inst. of Physics, New York, 2000, pp. 419–422.
[36] T.J. Ressler, J. Sync. Rad. 5 (1998) 118.
[37] F.W. Lytle, D.E. Sayers, E.A. Stern, Phys. B 158 (1989) 701.
[38] M. Vaarkamp, F.S. Modica, J.T. Miller, D.C. Koningsberger, J. Catal. 144 (1993) 611.
[39] D. Bazin, A. Triconnet, P. Moureaux, Nucl. Instrum. Methods Phys. Res. B 97 (1–4) (1995) 41.
[40] R.B. Greegor, F.W. Lytle, J. Catal. 63 (1980) 476–486.
[41] A.I. Frenkel, C.W. Hills, R.G. Nuzzo, J. Phys. Chem. B 105 (2001) 12689–12703.
[42] R.K. Herz, E.J. Shinouskis, Appl. Surf. Sci. 19 (1984) 373–397.
[43] J.A. Anderson, J. Chem. Soc., Faraday Trans. 88 (8) (1992) 1197–1201.
[44] X. Xu, J. Szanyi, Q. Xu, D.W. Goodman, Catal. Today 21 (1994) 57–69.
[45] L. Piccolo, C. Becker, C.R. Henry, Eur. Phys. J. D 9 (1999) 415–419.
[46] M. Mavrikakis, P. Stoltze, J.K. Norskov, Catal. Lett. 64 (2–4) (2000) 101–106.
[47] F. Gracia, E.E. Wolf, Chem. Eng. J. 82 (2001) 291–301.
[48] F. Gracia, E.E. Wolf, 2003, to be submitted.
[49] J. Siera, R. Van Silfhout, F. Rutten, B.E. Nieuwenhuys, Stud. Surf. Sci. Catal. 71 (1991) 395–407.